



The Cellular Basis of GABA_B-Mediated Interhemispheric Inhibition

Lucy M. Palmer *et al.*
Science **335**, 989 (2012);
DOI: 10.1126/science.1217276

This copy is for your personal, non-commercial use only.

If you wish to distribute this article to others, you can order high-quality copies for your colleagues, clients, or customers by [clicking here](#).

Permission to republish or repurpose articles or portions of articles can be obtained by following the guidelines [here](#).

The following resources related to this article are available online at www.sciencemag.org (this information is current as of June 16, 2012):

Updated information and services, including high-resolution figures, can be found in the online version of this article at:

<http://www.sciencemag.org/content/335/6071/989.full.html>

Supporting Online Material can be found at:

<http://www.sciencemag.org/content/suppl/2012/02/23/335.6071.989.DC1.html>

A list of selected additional articles on the Science Web sites **related to this article** can be found at:

<http://www.sciencemag.org/content/335/6071/989.full.html#related>

This article **cites 33 articles**, 16 of which can be accessed free:

<http://www.sciencemag.org/content/335/6071/989.full.html#ref-list-1>

This article appears in the following **subject collections**:

Neuroscience

<http://www.sciencemag.org/cgi/collection/neuroscience>

28. W. Tian *et al.*, *Cell. Immunol.* **234**, 39 (2005).
 29. M. J. Dobrzanski, J. B. Reome, J. A. Hollenbaugh, R. W. Dutton, *J. Immunol.* **172**, 1380 (2004).
 30. L. A. Koopman *et al.*, *J. Exp. Med.* **198**, 1201 (2003).
 31. N. S. Joshi *et al.*, *Immunity* **27**, 281 (2007).
 32. A. H. Rahman *et al.*, *Blood* **117**, 3123 (2011).
 33. S. N. Mueller *et al.*, *Proc. Natl. Acad. Sci. U.S.A.* **104**, 15430 (2007).
 34. S. Gallucci, P. Matzinger, *Curr. Opin. Immunol.* **13**, 114 (2001).
 35. R. Le Goffic *et al.*, *Am. J. Respir. Cell Mol. Biol.* **45**, 1125 (2011).
 36. A. Becerra, R. V. Warke, N. de Bosch, A. L. Rothman, I. Bosch, *Cytokine* **41**, 114 (2008).
 37. O. Joffre, M. A. Nolte, R. Spörri, C. Reis e Sousa, *Immunol. Rev.* **227**, 234 (2009).
- Acknowledgments:** This work was supported by Bundesministerium für Bildung und Forschung (BMBF)—FORSYS (A.F., M.L.), National Health and Medical Research Council (S.J.), German Research Foundation (GRK1121, A.N.H.), Science Foundation Ireland (P.G.F.), Program for Improvement of Research Environment for Young Researchers, the Special Coordination Funds for Promoting Science and Technology from the Japanese Ministry of Education, Culture, Sports, Science and Technology, Japan Science and Technology Agency, PRESTO (S.N.), BMBF (NGFNplus, FKZ PIM-01GS0802-3; H.A.), Wilhelm Sander-Stiftung (H.A.), German Research Foundation (SFB618 and SFB650, M.L.), Volkswagen Foundation (Lichtenberg Program, M.L.), Fondation Leenaards (D.D.P.), European Community (D.D.P.), and Swiss National Science Foundation (D.M., D.D.P.). We thank A. Berghaler, G. R. Burmester, C. Gabay, M. Geuking, A. Kamath, P. H. Lambert, J. Luban, B. Marsland, G. Palmer, A. Radbruch, C. A. Siegrist, and R. M. Zinkernagel for discussions and advice; H. Saito, National Research Institute for Child Health and Development, for *IL33*^{-/-} mice obtained under a materials transfer agreement (MTA) through the RIKEN Center for Developmental Biology, Laboratory for Animal Resources and Genetic Engineering; A. McKenzie (for *IL1rl1*^{-/-} mice obtained under MTA); the University of Zurich (for rLCMV technology obtained under MTA) and G. Jennings [Cytos Biotechnology AG, Schlieren, Switzerland, holding patent rights on VLPs provided] for reagents; and J. Weber and B. Steer

for technical assistance. The data presented in this paper are tabulated in the main paper and the supporting online material. Microarray data are deposited with National Center for Biotechnology Information Gene Expression Omnibus (GEO), accession number GSE34392 and ArrayExpress (accession number E-MTAB-901). D.D.P. is or has been a shareholder, board member, and consultant to ArenaVax AG, Switzerland, and to Hookipa Biotech GmbH, Austria, commercializing rLCMV vectors (patent application EP 07 025 099.8, coauthored by D.D.P.). The authors declare that they do not have other competing financial interests.

Supporting Online Material

www.sciencemag.org/cgi/content/full/science.1215418/DC1
 Materials and Methods
 Figs. S1 to S4
 Tables S1 and S2
 References (38–40)

18 October 2011; accepted 20 January 2012
 Published online 9 February 2012;
 10.1126/science.1215418

The Cellular Basis of GABA_B-Mediated Interhemispheric Inhibition

Lucy M. Palmer,¹ Jan M. Schulz,¹ Sean C. Murphy,¹ Debora Ledergerber,¹ Masanori Murayama,² Matthew E. Larkum^{1,3*}

Interhemispheric inhibition is thought to mediate cortical rivalry between the two hemispheres through callosal input. The long-lasting form of this inhibition is believed to operate via γ -aminobutyric acid type B (GABA_B) receptors, but the process is poorly understood at the cellular level. We found that the firing of layer 5 pyramidal neurons in rat somatosensory cortex due to contralateral sensory stimulation was inhibited for hundreds of milliseconds when paired with ipsilateral stimulation. The inhibition acted directly on apical dendrites via layer 1 interneurons but was silent in the absence of pyramidal cell firing, relying on metabotropic inhibition of active dendritic currents recruited during neuronal activity. The results not only reveal the microcircuitry underlying interhemispheric inhibition but also demonstrate the importance of active dendritic properties for cortical output.

The connection between the two hemispheres of the cerebral cortex via the corpus callosum is one of the most studied and yet least understood pathways in the brain (1, 2). An important function of transcallosal fibers is to mediate interhemispheric inhibition (3, 4), which influences fine motor control (5, 6), visuospatial attention (7–9), and somatosensory processing (10, 11). To investigate the cellular mechanisms of interhemispheric inhibition, we performed in vivo patch-clamp recordings from layer 5 (L5) pyramidal neurons in the hindlimb area of the somatosensory cortex in urethane-anesthetized rats (Fig. 1A). Stimulation of the contralateral hindpaw (contralateral HS) (1-ms duration, 100 V) increased the baseline firing rate by a factor of about 3 (0.9 ± 0.2 to 2.9 ± 0.6 Hz; $P < 0.05$; $n = 19$)

(Fig. 1, B to D, black). Ipsilateral hindpaw stimulation (ipsilateral HS), on the other hand, had little influence on the firing rate (1-ms duration, 100V; spontaneous, 1.1 ± 0.2 Hz and evoked, 1.2 ± 0.2 Hz; $n = 19$ (Fig. 1B, green). However, an inhibitory influence of ipsilateral HS could be uncovered by pairing it with contralateral HS (paired HS). Here, paired HS resulted in a significant decrease in evoked firing (evoked, 2.2 ± 0.5 Hz; $n = 19$; $P < 0.05$) when the ipsilateral hindpaw was stimulated 400 ms before the contralateral hindpaw (Fig. 1, B to D, blue). This influence of paired HS on action potential (AP) generation occurred throughout the entire evoked excitatory response, which lasted on average 513 ± 49 ms ($n = 19$) (Fig. 1C, gray area). Unexpectedly, paired HS had no discernible effect on the subthreshold responses (Fig. 1, B to D), which did not significantly decrease in average area (3.4 ± 0.6 versus 3.4 ± 0.6 mV*s; $n = 20$) nor variance (15.7 ± 1.9 versus 17.2 ± 0.2 mV²; $n = 20$) (fig. S1).

The average $25 \pm 8\%$ decrease in the evoked firing during paired HS was somatotopically specific because stimulation of different regions

of the body, or even different parts of the hindlimb, did not reduce the response to contralateral HS (fig. S2). Furthermore, the decrease in firing did not occur when the contralateral hindpaw was stimulated twice at an interval of 400 ms (fig. S3), and paired HS had no inhibitory effect on layer 2/3 (L2/3) pyramidal neurons (contralateral HS, 3.9 ± 0.6 Hz; paired HS, 3.6 ± 0.7 Hz; $t = 400$ ms; $n = 9$) (fig. S4). When the timing of the paired-HS interval was varied in 200-ms steps, L5 pyramidal neuron firing was only influenced when the ipsilateral hindpaw was stimulated either 200 or 400 ms before the contralateral hindpaw (Fig. 1E). The long-time course for this type of inhibition suggested the involvement of γ -aminobutyric acid type B (GABA_B) receptors, which can exert an effect for up to 500 ms in vitro (12). Indeed, application of the GABA_B-receptor antagonist, CGP52432 (1 μ M) to the cortical surface blocked the decrease in firing generated by paired HS (contralateral HS, 1.9 ± 0.7 Hz; paired HS, 2.0 ± 0.9 Hz, $t = 400$ ms; $n = 8$) (Fig. 1E).

It has been suggested in humans that ipsilateral somatosensory stimulation leads to suppression of sensory responses due to transcallosal inhibition (13). We tested this hypothesis in rats using optogenetic stimulation of the transcallosal pathway in vivo. Deep-layer neurons infected with channelrhodopsin-2 (ChR2) conjugated with adenovirus (AAV) sent callosal fibers predominantly to the upper layers of the opposite hemisphere (Fig. 2A) and fig. S5 [see supporting online material (SOM)]. Photostimulation (470 nm; trains of 10- by 10-ms pulses at 10 Hz, beginning 400 ms before the sensory stimulus) of callosal input decreased the evoked firing rate of L5 pyramidal neurons by $36 \pm 15\%$ when the light was focused above the hemisphere containing the recording electrode ($n = 9$; $P < 0.05$) (Fig. 2, B and C) and by $38\% \pm 14\%$ with photostimulation of the injected hemisphere ($n = 7$; $P < 0.05$) (fig. S6). Photoactivation of the callosal fibers alone did not influence spontaneous firing activity (0.6 ± 0.2 Hz prephotoactivation and 0.7 ± 0.3 Hz during photoactivation) (fig. S6), and there was

¹Physiologisches Institut, Universität Bern, Bühlpplatz 5, CH-3012 Bern, Switzerland. ²Behavioral Neurophysiology Laboratory, Brain Science Institute, Riken, 2-1 Hirosawa, Wako, Saitama 351-0198, Japan. ³Neurocare Cluster of Excellence, Department of Biology, Humboldt University, Charitéplatz 1, 10117, Berlin, Germany.

*To whom correspondence should be addressed. E-mail: matthew.larkum@gmail.com

no measurable influence of callosal fiber photo-activation on the underlying subthreshold envelope (contralateral HS alone, 2.1 ± 0.5 mV•s compared with contralateral HS + ChR2, 2.5 ± 0.5 mV•s; $P > 0.05$; $n = 13$) (fig. S6).

The corpus callosum consists almost entirely of excitatory fibers (14), which implies that interhemispheric inhibition arises from the activation of local interneurons. We tested this *ex vivo* with photostimulation of callosal fibers while recording from local interneurons in brain slices prepared from rats previously injected with ChR2/AAV (Fig. 2, A and D). To investigate monosynaptic callosal input, we added TTX (1 μ M) and 4-AP (100 μ M) (15) and activated callosal fibers using 460-nm light pulses over the field of view (10 by 10-ms pulses at 10 Hz, 60X objective). Interneurons were identified by their morphology and spiking characteristics (16) (fig. S7). The voltage response to monosynaptic callosal input in interneurons located in L1 (29.1 ± 6.6 mV; $n = 9$) and L2/3 (31.1 ± 4.6 mV; $n = 20$) was significantly larger than L5 interneurons (14.4 ± 3.5 mV; $n = 24$; $P < 0.05$) (Fig. 2, E and F). To further investigate the laminar specificity of callosal input on interhemispheric inhibition, we locally perfused the excitatory AMPA-receptor antagonist CNQX (100 μ M) above the recorded cell *in vivo*. Interhemispheric inhibition evoked with paired HS was completely abolished by CNQX perfused into L1 (paired HS/contralateral HS 1.0 ± 0.1 ; $n = 6$) but not L2/3 (paired HS/contralateral HS, 0.6 ± 0.1 ; $n = 6$) (Fig. 2, G and H), suggesting that callosal input to L1 is crucial (see also fig. S8). (Local perfusion of CNQX did not in itself significantly change the AP firing rate of L5 pyramidal neurons in response to contralateral HS). In contrast to pyramidal neurons

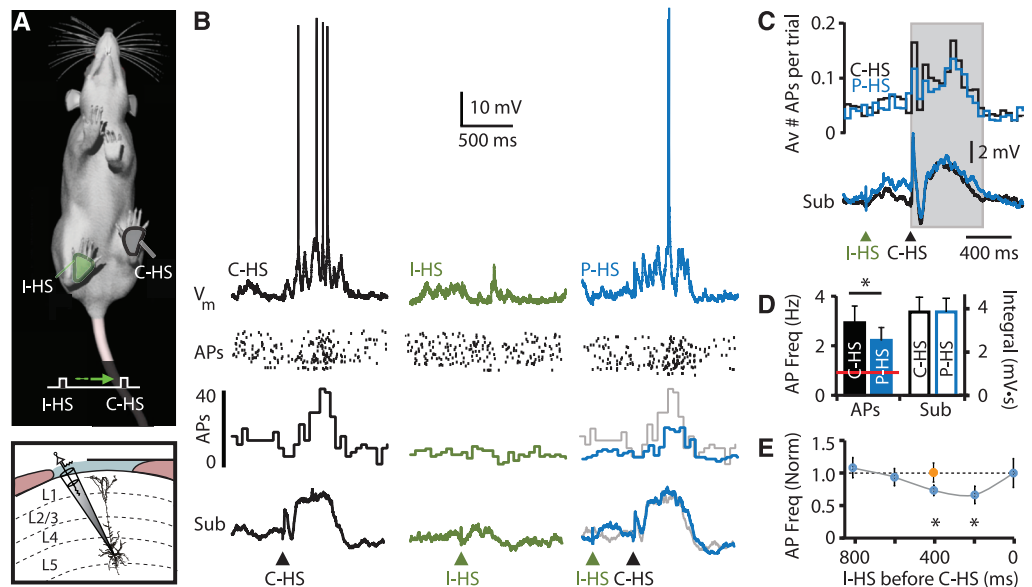
(Fig. 1B), ipsilateral HS alone evoked activity in L1 neurons. Two-photon calcium imaging from L1 neurons bulk-loaded with the calcium indicator Oregon Green 488 BAPTA-1-AM (OGB-1-AM) (Fig. 2I) revealed responses to ipsilateral HS in 41% of L1 neurons (Fig. 2J) ($n = 107$ neurons from seven rats). L1 contains a subpopulation of late-spiking, neurogliaform cells (~40% of cells) (17) that provide GABA_B-mediated inhibition (18) to the dendrites of pyramidal neurons (19).

The targeting of callosal input to L1 suggests that interhemispheric inhibition of L5 pyramidal neurons may act through a dendritically located mechanism (12, 19, 20). We therefore investigated the effects of ipsilateral HS on the calcium response in a population of L5 pyramidal neuron dendrites using a fiberoptic technique for recording dendritic activity (the “periscope” system) (21, 22) (Fig. 3A) (see SOM). Contralateral HS evoked a biphasic Ca²⁺ signal in L5 pyramidal neuron dendrites (Fig. 3B, black trace) that was significantly reduced ($31 \pm 6\%$; $P < 0.05$) when paired with ipsilateral HS ($t = 400$ ms; $n = 13$) (blue trace, Fig. 3, B and C) (see fig. S9 for times all between $t = 0$ and $t = 800$ ms). This decrease in dendritic activity was abolished by application of the GABA_B-receptor antagonist CGP52432 (1 μ M) to the cortical surface (Fig. 3C, right). The similar inhibitory influence of paired HS on firing rates and dendritic Ca²⁺ in L5 pyramidal neurons suggests a strong correlation between dendritic activity and somatic output *in vivo*.

Was the down-regulation of dendritic Ca²⁺ activity due to the pre- or postsynaptic activation of dendritic GABA_B receptors (12) that are abundant in pyramidal apical dendrites (23)? We used three strategies to investigate this ques-

tion. First, we recorded dendritic Ca²⁺ activity with the periscope while focally applying the GABA_B agonist baclofen (50 μ M) to the distal apical dendrites of L5 pyramidal neurons *in vivo* (Fig. 3D). We observed an even larger decrease in the area ($55 \pm 9\%$; $n = 8$) and amplitude ($51 \pm 6\%$; $n = 8$) of the evoked dendritic Ca²⁺ response (Fig. 3, E and F). Second, we performed whole-cell recordings from L5 dendrites identified by their distinctive complex AP waveforms (24) (fig. S10) and post hoc biocytin reconstructions (Fig. 3G) (see SOM). During baclofen applied either focally to the distal dendrite or on the cortical surface, the dendritic response to contralateral HS decreased by ~75% from 1.75 ± 0.3 Hz to 0.4 ± 0.2 Hz ($n = 5$; average dendritic patch distance, 943 ± 34 μ m from the pia) (Fig. 3, H and I). Last, we recorded electrical activity at the soma *in vivo* (as in Fig. 1) in knockout mice that lacked GABA_B receptor isoforms known to act presynaptically (GABA_{B1a}^{-/-}) and postsynaptically (GABA_{B1b}^{-/-}) in L5 pyramidal neurons (12, 25) (Fig. 3J). In mice lacking the postsynaptically acting isoform (GABA_{B1b}^{-/-}), we recorded no interhemispheric inhibition using paired HS (7.6 ± 1.8 Hz versus 8.7 ± 1.9 Hz; $t = 400$ ms; $n = 7$) (Fig. 3K), whereas the inhibition remained in mice lacking the presynaptically acting isoform (GABA_{B1a}^{-/-}; 10.0 ± 4.9 Hz versus 6.1 ± 3.9 Hz; $t = 400$ ms; $n = 4$) (Fig. 3L). Furthermore, the inhibitory effect of focal application of baclofen to the dendrites was also occluded in GABA_{B1b}^{-/-} mice (9.0 ± 2.3 versus 12.0 ± 4.5 Hz; $n = 5$) (Fig. 3, K and L). The specificity of the effect to GABA_{B1b} receptors and the observed effects on dendritic Ca²⁺ strongly suggest that interhemispheric inhibition is mediated by dendritically located GABA_B receptors.

Fig. 1. Interhemispheric inhibition of sensory information. **(A)** Experimental design. (Top) Electrical stimulation (100 V, 1 ms), of contralateral and ipsilateral hindpaws during patch-clamp recordings from L5 pyramidal neurons (bottom). **(B)** (Top) Somatic response, (middle) raster plot and histogram of total AP firing over multiple trials, and (bottom) average subthreshold response in trials during contralateral HS (C-HS) (black; left), ipsilateral HS (I-HS) (green; middle), and paired HS (P-HS) (blue). I-HS 400 ms before C-HS (right). Gray traces, C-HS for comparison. **(C)** (Top) AP histogram for C-HS (black) and P-HS ($t = 400$ ms; blue) across all neurons (bin width = 50 ms; $n = 19$). (Bottom) Grand mean subthreshold responses to C-HS (black) and P-HS (blue; $n = 20$). Gray region used for statistics. **(D)** (Left) Average AP frequency during C-HS (black) and P-HS (blue; solid bars; $n = 19$). Red line, spontaneous firing rate. (Right) Average subthreshold response to C-HS (black) and P-HS (blue; $n = 20$; open bars). **(E)** Average normalized AP frequency during P-HS with I-HS 0, 200, 400, 600,



and 800 ms before C-HS (blue dots). Orange dot, normalized average AP frequency during P-HS ($t = 400$ ms) with GABA_B antagonist CGP52432 applied to cortical surface. *, $P < 0.05$.

Fig. 2. Callosal fiber activation inhibits L5 pyramidal neuron firing and activates L1 neurons. **(A)** (Top) Experimental design. ChR2/AAV injected into hindlimb somatosensory cortex before patch recording in opposite hemisphere. (Middle) Overlays of bright-field images and ChR2 fluorescence from injected (left) and recording hemispheres (right) ex vivo. (Bottom) In vivo 2P image of ChR2 axons (green) in recording hemisphere at 100 μ m below pia. **(B)** (Top) Somatic response, (middle) raster plot, and (bottom) histogram of APs during C-HS alone (left) and photostimulation with train of blue-light pulses above recording hemisphere (right). **(C)** Average firing frequency with C-HS (black) and during photostimulation of recording hemisphere (aqua; +ChR2). **(D)** Ex vivo recording from interneurons in L1, L2/3, and L5 in slices from ChR2/AAV-injected rats. **(E)** Voltage responses to local photostimulation in L1 (green), L2/3 (maroon), and L5 (turquoise). L1 and L5 interneurons recorded simultaneously; interneurons shown in **(D)**. **(F)** Average voltage response to first photostimulation. **(G)** Example voltage response, raster plot, and AP histogram with (top) C-HS and (bottom) P-HS with focal application of CNQX into L1. (Inset) Normalized firing rates with P-HS during control (blue), CNQX in L1 (pink), and CNQX in L2/3 (salmon). Shaded region used for statistics. **(H)** Average AP frequency during P-HS with CNQX in L1 and L2/3. **(I)** In vivo 2P image of L1 (<200 μ m below pia) counter-stained with OGB-1-AM and SR101. Neurons, green; astroglia, orange. **(J)** Individual (gray) and average (green) Ca^{2+} transients with I-HS for the cells in **(I)**. **(K)** Number of cells in L1 that responded (green) and did not respond (gray) to I-HS. *, $P < 0.05$.

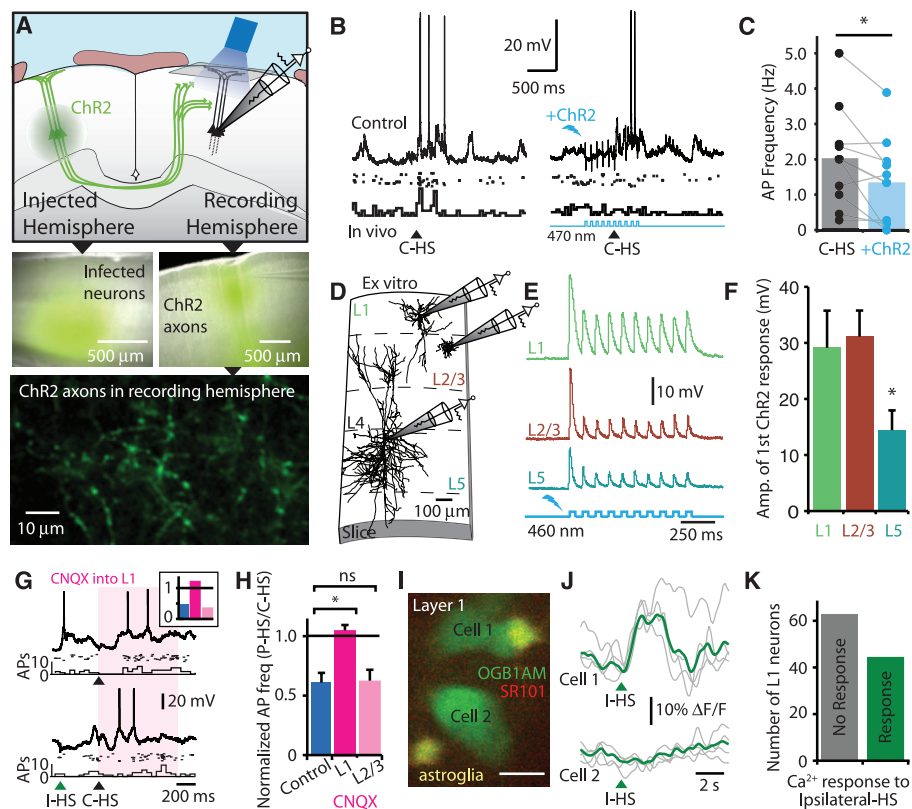
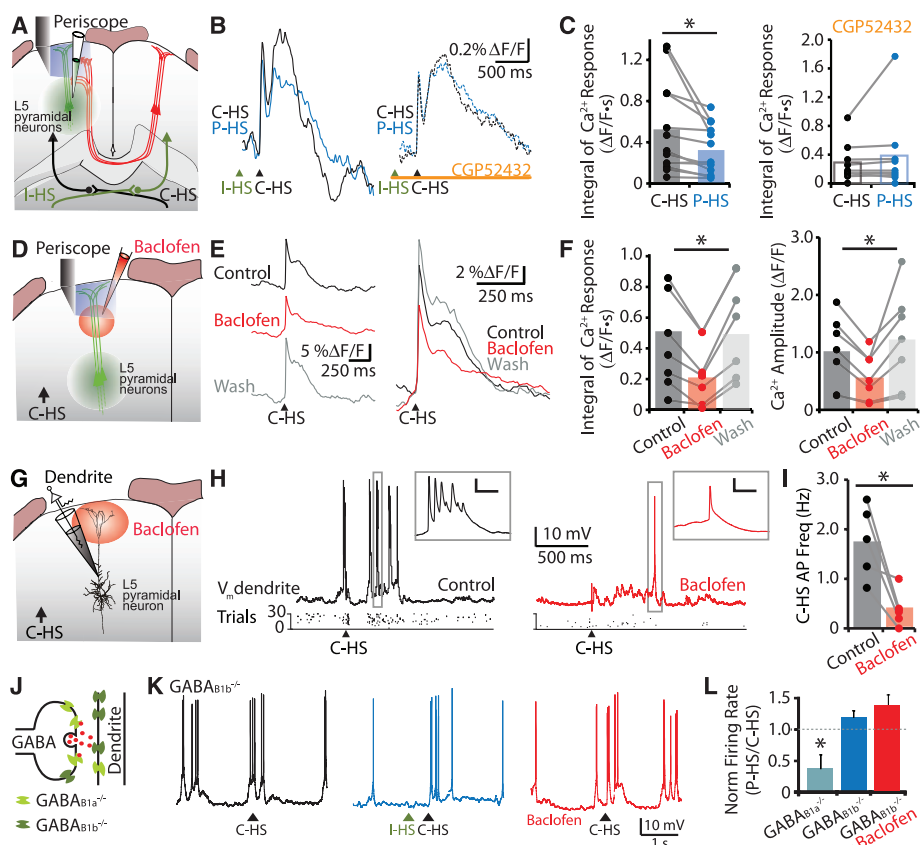


Fig. 3. Long-lasting interhemispheric inhibition is mediated by dendritic $GABA_B$ receptors. **(A)** Experimental design. L5 pyramidal neurons in the contralateral sensorimotor cortex bulk loaded with OGB-1-AM; dendritic Ca^{2+} responses recorded with periscope during C-HS and P-HS. **(B)** (Left) Average dendritic Ca^{2+} population response (fluorescence change, $\Delta F/F$; 15 trials) during C-HS (black) and P-HS (blue). (Right) Ca^{2+} response (10 trials) to C-HS (black) and P-HS (blue) during application of CGP52432 (1 μ M) to cortical surface. **(C)** (Left) Integral of the Ca^{2+} response to C-HS (black) and P-HS (blue) in control conditions and (right) during CGP52432. **(D)** Experimental design. **(E)** Average dendritic Ca^{2+} population response with C-HS before (black), during (red), and after (gray) baclofen application. **(F)** (Left) Integral and (right) amplitude of Ca^{2+} response to C-HS. **(G)** Experimental design: L5 dendritic patch during baclofen application. **(H)** Dendritic patch-clamp responses to C-HS before (black) and during (red) baclofen. (Inset) Complex waveform from boxed region. Scale bar, 10 mV, 10 ms. **(I)** Normalized firing rate in the dendrite to C-HS before (black) and during (red) baclofen. **(J)** Distribution of $GABA_B$ subunits pre- and postsynaptically. **(K)** Somatic voltage responses to C-HS (black), P-HS (blue), and C-HS during focal baclofen (50 μ M) application (red) in mice lacking postsynaptic $GABA_B$ receptors ($GABA_{B1b}^{-/-}$). **(L)** Normalized somatic firing rate during C-HS and P-HS in $GABA_{B1a}^{-/-}$ and $GABA_{B1b}^{-/-}$ mice. *, $P < 0.05$.



We next investigated how dendritic GABA_B receptors influence cell spiking in vivo. We repeated the experiments with focal dendritic baclofen application during somatic recordings from L5 pyramidal neurons (Fig. 4A). Baclofen decreased the evoked firing response by a similar amount to dendritic Ca²⁺ activity (64 ± 10%; n = 7) (Fig. 4, B and C) (compare Figure 3F). Despite this, baclofen (like interhemispheric inhibition) had no significant effect on the subthreshold electrical response at the soma (control, 3.6 ± 0.7 mV*s; baclofen, 3.0 ± 0.5 mV*s; n = 11) (Fig. 4, C and D). How could such profound effects on dendritic activity and cell firing occur in the absence of any detectable effect on membrane potential at the cell body?

To investigate this, we performed the same experiments in vitro where we could isolate the causes and effects to the dendritic and/or somatic compartments of the neuron (Fig. 4E). Activating dendritic GABA_B receptors continuously with baclofen resulted in an average hyperpolarizing response of only -1.2 ± 0.2 mV at the dendrite and -0.5 ± 0.2 mV at the soma (n = 19). Although this explained the negligible effect of dendritic GABA_B inhibition on the somatic subthreshold responses reported throughout this study, it made the large effect on cell firing even more intriguing. We hypothesized that sufficiently large dendritic depolarization activates dendritic voltage-sensitive channels that causes further AP firing. At subthreshold levels, dendritic depolarization would not be expected to activate voltage-sensitive channels, and thus dendritic inhibition of these channels would not be detected (i.e., silent inhibition).

To test this hypothesis, we recorded responses to contralateral HS in vivo from the soma and dendrites of L5 pyramidal neurons and used these recorded waveforms as representative current input in our somatic and dendritic recordings in vitro. Current was injected at the soma in increasing steps of 100 pA and at the dendrite at a fixed amount of 600 to 800 pA (Fig. 4F). For low somatic current injection (0 to 100 pA), there was little or no AP firing in the neuron (Fig. 4, G and H), and baclofen had little effect on either the membrane potential at the soma (Fig. 4G) or the input resistance of the neuron (Fig. 4, K and L). Higher somatic current injection led to cell firing and back-propagating APs into the apical dendrite. In this case, baclofen caused a significant decrease in firing rate (Fig. 4, F and H) and a decrease in the gain of the frequency/current relationship (26) (Fig. 4H, top). Under these suprathreshold conditions, the membrane potential at the soma (measured from the voltage envelope with APs truncated) was hyperpolarized during the application of baclofen relative to control (Fig. 4H, bottom) indicating a loss of current transfer from the dendrite to the soma. These results show conclusively that dendritic GABA_B inhibition alone can significantly reduce the firing output of L5 pyramidal neurons through a dendritically located mechanism that manifests only when the neuron is spiking.

To further investigate the importance of dendritic activity on somatic output, we restricted current injection to the soma while continuing to apply baclofen locally to the dendrite (Fig. 4I). Even with no dendritic input at all, activation of

dendritic GABA_B receptors still caused a significant decrease in AP firing rate (by 38 ± 5%, n = 11) (Fig. 4, J and L). Furthermore, the decrease in APs during GABA_B receptor activation was not caused predominately by shunting inhibition

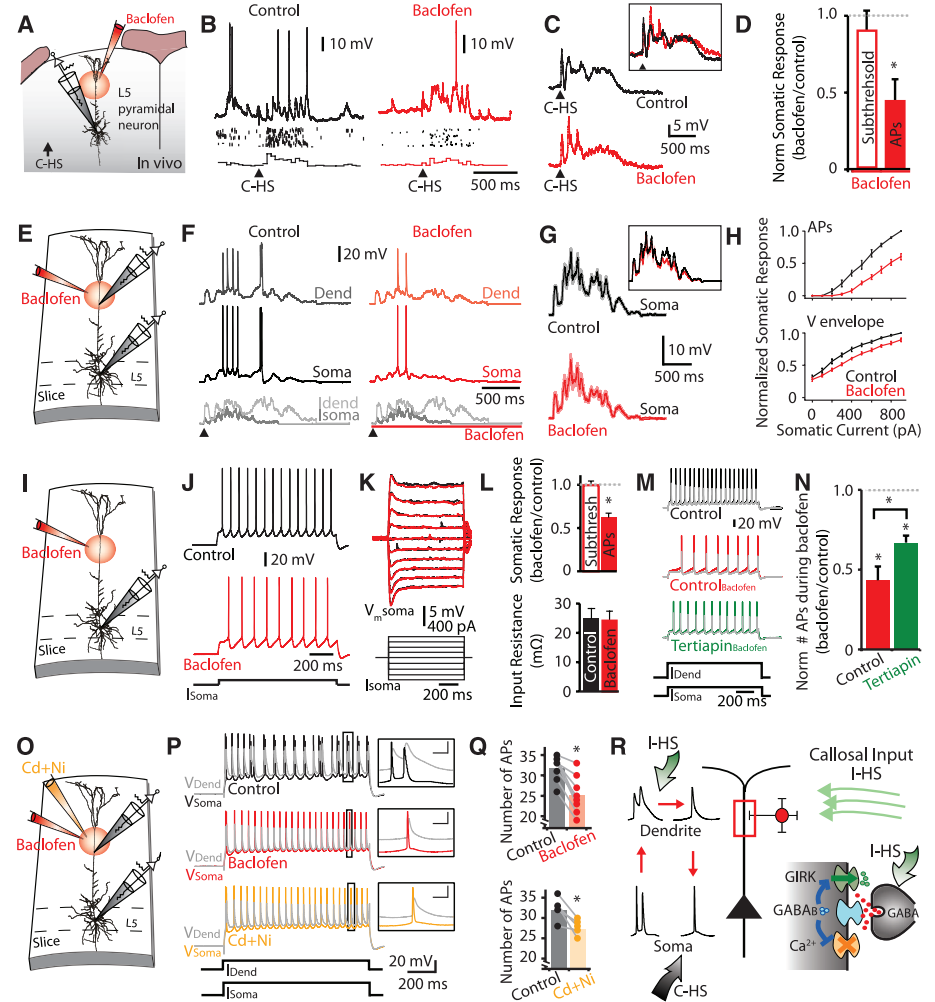


Fig. 4. The dendritic mechanisms of interhemispheric inhibition. **(A)** Experimental design. **(B)** Response to C-HS in control (black) and baclofen (red). **(C)** Average subthreshold response to C-HS. (Inset) Overlaid traces. **(D)** Average normalized response to C-HS under baclofen for the subthreshold voltage integral (open bar) and AP frequency (solid bar). **(E)** Experimental design. **(F)** (Top) Dendritic and somatic recordings in vivo with (bottom) waveforms injected into dendrite (light gray) and soma (dark gray). **(G)** Grand mean of the somatic subthreshold voltage responses to dual current injection shown in (F). (Inset) Overlaid traces. **(H)** Normalized somatic (top) firing rate and (bottom) voltage envelope integral evoked by constant dendritic and increasing somatic current injections during control (black) and baclofen (red). **(I)** Experimental design. **(J)** Somatic voltage response to suprathreshold current injection (400 pA) at soma. **(K)** Subthreshold voltage responses (top) to somatic current steps (bottom; 100 pA steps) before (black) and during (red) baclofen. **(L)** (Top) Normalized somatic subthreshold response (open bar) and number of APs (solid bar) during baclofen. (Bottom) Input resistance of the subthreshold somatic response during control (black) and baclofen (red). **(M)** Dual somatic (color) and dendritic (gray) voltage responses to current step injections (800 pA and 400 pA injected into the dendrite and soma, respectively) with (red) baclofen and (green) tertiapin (0.5 μM) in the bath solution. **(N)** Normalized number of APs evoked for (M). **(O)** Experimental design. **(P)** Dual somatic/dendritic responses to current injections (800 pA and 1200 pA injected into the dendrite and soma, respectively) before (black) and during (red) baclofen or Cd + Ni (yellow). (Inset) Boxed region on left. Scale bar, 20 mV, 100 ms. **(Q)** Number of APs in (P). **(R)** Proposed cellular mechanism of interhemispheric inhibition. C-HS generates dendritic input and back-propagating APs, which activate dendritic voltage-sensitive channels leading to more APs. I-HS activates GABA_B-mediating L1 interneurons that open GIRK and block Ca²⁺ channels (silent inhibition), which is only effective with dendritic depolarization from paired C-HS. *, P < 0.05 significance level.

because the same application of baclofen had no effect on the input resistance of the cell (Fig. 4, K and L).

What is the cellular basis of this GABA_B-mediated inhibition? Previous studies have shown that GABA_B inhibition leads to activation of inward-rectifying K⁺ channels (GIRK) (27) and inactivation of voltage-sensitive Ca²⁺ channels (12) in pyramidal neurons. Bath application of the GIRK antagonist tertiapin (0.5 μM) led to a 61 ± 11% decrease in the baclofen-induced hyperpolarization in the dendrite in vitro (*n* = 10) (fig. S11). Under these conditions, the inhibitory effect of baclofen on AP firing measured near threshold was partially occluded (control, 57 ± 9% versus tertiapin, 33 ± 5% reduction, respectively; average dendritic recording distance, 397 ± 2 μm) (Fig. 4, M and N). To determine the contribution of voltage-sensitive Ca²⁺ currents, we locally applied 50 μM Cd²⁺ and 100 μM Ni²⁺ to the apical dendrite at the same location as baclofen (Fig. 4O). Enough current was injected at the soma and dendrite to evoke firing well above threshold and maximize dendritic voltage-sensitive current activation. Ca²⁺ channel blockade accounted for 60 ± 18% (*n* = 5) of the reduction in AP firing induced by application of baclofen (average dendritic recording distance, 478 ± 36 μm) (Fig. 4, P and Q). In contrast to the GIRK channel antagonist, bath application of Ca²⁺ channel antagonists significantly reduced dendritic regenerative potentials and burst firing patterns (28) and occluded any further effect of baclofen on the spike waveform (fig. S12).

The dependence of dendritic GABA_B inhibition on suprathreshold dendritic depolarization explains why this form of inhibition is normally silent. During contralateral HS, dendritic voltage-sensitive currents contribute to the overall depolarization of the neuron and, although blocked by GABA_B receptor activation during ipsilateral HS, no inhibitory effect is measured because these currents are not activated without dendritic depolarization (e.g., due to dendritic input and/or back-propagating APs). Only with paired HS is the effect of regulating dendritic channel activity revealed (Fig. 4R). The magnitude of the effects observed in vitro would be sufficient to explain all of the effects seen in vivo. Although callosal

inhibition could also affect pyramidal cell firing through network effects that alter synaptic input, we did not detect a change in subthreshold responses during interhemispheric inhibition (Fig. 1). We conclude, therefore, that interhemispheric inhibition is mediated predominantly through direct postsynaptic mechanisms in the apical dendritic shafts of pyramidal neurons.

It has been suggested that interhemispheric inhibition might regulate the gain of synaptic input (29) and thereby serve to enhance bimanual precision (5, 30). Furthermore, loss of interhemispheric rivalry (through callosal inhibition) has been implicated in cases of lateralized impairment of attention (hemineglect) in human patients (9). Unraveling the mechanisms behind interhemispheric inhibition might therefore be critical to understanding these complex tasks. Our results reveal that long-lasting interhemispheric inhibition acts via a specific cortical microcircuitry mediated by dendritic GABA_B receptors. This phenomenon of silent inhibition of dendritic channels, however, is likely to be a general phenomenon under many different conditions and may therefore represent a novel mechanism for explaining the anomalous decoupling of subthreshold and suprathreshold activity seen in other systems in vivo (31–34). The specific mechanisms of interhemispheric inhibition shown here, involving the underlying cortical microcircuitry, and dendritic GABA_B receptors, offer new perspectives on fundamental and clinical studies involving interactions between the two cortical hemispheres.

References and Notes

- M. S. Gazzaniga, *Nat. Rev. Neurosci.* **6**, 653 (2005).
- J. S. Bloom, G. W. Hynd, *Neuropsychol. Rev.* **15**, 59 (2005).
- H. Asanuma, O. Okuda, *J. Neurophysiol.* **25**, 198 (1962).
- A. Ferbert *et al.*, *J. Physiol.* **453**, 525 (1992).
- G. M. Geffen, D. L. Jones, L. B. Geffen, *Behav. Brain Res.* **64**, 131 (1994).
- M. Kobayashi, S. Hutchinson, H. Théoret, G. Schlaug, A. Pascual-Leone, *Neurology* **62**, 91 (2004).
- K. M. Heilman, E. Valenstein, *Neurology* **22**, 660 (1972).
- C. C. Hilgetag, H. Théoret, A. Pascual-Leone, *Nat. Neurosci.* **4**, 953 (2001).
- D. Cazzoli, P. Wurtz, R. M. Müri, C. W. Hess, T. Nyffeler, *Eur. J. Neurosci.* **29**, 1271 (2009).
- M. Seyal, T. Ro, R. Rafal, *Ann. Neurol.* **38**, 264 (1995).
- N. Forss, M. Hietanen, O. Salonen, R. Hari, *Brain* **122**, 1889 (1999).

- E. Pérez-Garci, M. Gassmann, B. Bettler, M. E. Larkum, *Neuron* **50**, 603 (2006).
- Y. Hlushchuk, R. Hari, *J. Neurosci.* **26**, 5819 (2006).
- G. M. Innocenti, in *Cerebral Cortex*, E. G. Jones, A. Peters, Eds. (Plenum Press, New York, 1986), vol. 5, pp. 291–353.
- L. Petreanu, D. Huber, A. Sobczyk, K. Svoboda, *Nat. Neurosci.* **10**, 663 (2007).
- G. A. Ascoli *et al.*; Petilla Interneuron Nomenclature Group, *Nat. Rev. Neurosci.* **9**, 557 (2008).
- Z. Chu, M. Galarreta, S. Hestrin, *J. Neurosci.* **23**, 96 (2003).
- G. Tamás, A. Lörincz, A. Simon, J. Szabadics, *Science* **299**, 1902 (2003).
- C. Wozny, S. R. Williams, *Cereb. Cortex* **21**, 1818 (2011).
- H. G. Kim, M. Beierlein, B. W. Connors, *J. Neurophysiol.* **74**, 1810 (1995).
- M. Murayama, E. Pérez-Garci, H. R. Lüscher, M. E. Larkum, *J. Neurophysiol.* **98**, 1791 (2007).
- M. Murayama *et al.*, *Nature* **457**, 1137 (2009).
- G. López-Bendito *et al.*, *Eur. J. Neurosci.* **15**, 1766 (2002).
- F. Helmchen, K. Svoboda, W. Denk, D. W. Tank, *Nat. Neurosci.* **2**, 989 (1999).
- B. Bettler, K. Kaupmann, J. Mosbacher, M. Gassmann, *Physiol. Rev.* **84**, 835 (2004).
- M. E. Larkum, W. Senn, H. R. Lüscher, *Cereb. Cortex* **14**, 1059 (2004).
- N. R. Newberry, R. A. Nicoll, *Nature* **308**, 450 (1984).
- S. Williams, G. Stuart, *J. Physiol.* **521**, 161 (1999).
- A. Schnitzler, K. R. Kessler, R. Benecke, *Exp. Brain Res.* **112**, 381 (1996).
- C. Gerloff, F. G. Andres, *Acta Psychol. (Amst.)* **110**, 161 (2002).
- V. Bringuier, F. Chavane, L. Glaeser, Y. Frégnac, *Science* **283**, 695 (1999).
- M. Carandini, D. Ferster, *J. Neurosci.* **20**, 470 (2000).
- M. Brecht, B. Sakmann, *J. Physiol.* **538**, 495 (2002).
- H. Jia, N. L. Rochefort, X. Chen, A. Konnerth, *Nature* **464**, 1307 (2010).

Acknowledgments: We thank B. Bettler, J. Seibt, E. Pérez-Garci, T. Nyffeler, R. Müri and H. -R. Lüscher for their helpful comments on the manuscript. We also thank B. Bettler and M. Gassman for kindly providing the knockout mice (GABA_{B1a}^{-/-} and GABA_{B1b}^{-/-}) and N. Nevia for technical assistance. This work was supported by SystemsX.ch (NeuroChoice) and the Swiss National Science Foundation (PP00A-102721 and 31003A_130694).

Supporting Online Material

www.sciencemag.org/cgi/content/full/335/6071/989/DC1

Materials and Methods

SOM Text

Figs. S1 to S12

References

30 November 2011; accepted 18 January 2012

10.1126/science.1217276